Math. Proc. Camb. Phil. Soc. (1977), **82**, 147
With 14 text-figures and 1 plate
Printed in Great Britain

On Legendre transformations and elementary catastrophes

By M. J. SEWELL
Department of Mathematics, University of Reading

(*Received* 17 *November* 1976)

1. *Introduction.* The purpose of these remarks is to use elementary mathematics to describe some simple connexions between multi-valued Legendre transformations and certain elementary catastrophes. Multi-valued Legendre transforms appear in subjects such as non-linear elasticity and non-convex optimization.

2. *Some simple Legendre transforms.* Consider the general polynomial equation in x of the nth degree. This can be written, after normalizing the leading coefficient, as

$$u = x^n + tx^{n-1} + \ldots + bx^2 + ax,$$

where the coefficients are then $a, b, \ldots, t, u$. Now express this in the alternative gradient form

$$u = dX/dx, \tag{1}$$

where the generating potential function $X(x)$ is defined by

$$X = \frac{1}{n+1}x^{n+1} + \frac{t}{n}x^n + \ldots + \frac{b}{3}x^3 + \frac{a}{2}x^2.$$

Recall that such a polynomial equation has either 0 or 2 or ... or n real roots if n is even, and either 1 or 3 or ... or n real roots if n is odd.

Those points of the potential function $X(x)$ which satisfy

$$d^2X/dx^2 = 0 \tag{2}$$

can be divided into two sets, according to whether the lowest value of $r > 2$ which makes

$$d^rX/dx^r \neq 0 \tag{3}$$

is (a) odd or (b) even.

(a) These points are inflexion points of $X(x)$, because the *slope* of $X(x)$ attains a stationary local minimum or maximum as it passes through such a point, by the Taylor expansion.

(b) These points are not inflexion points because the slope of $X(x)$ only becomes stationary at such a point, and then resumes its previous monotonically increasing or decreasing character. The simplest example is the increasing slope of $X(x) = x^4$ on both sides of $x = 0$, where the lowest value of r is 4.

If the normalized constant u in the original polynomial is now regarded as a controllable parameter, equation (1) can be viewed as a mapping

$$u = u(x)$$

of a real x-axis onto a real u-axis. As x passes through a point where (2) holds, the

https://doi.org/10.1017/S0305004100053779 Published online by Cambridge University Press

corresponding point on the u-axis will reverse direction for a point of type (a) (i.e. for an inflexion point of $X(x)$); but for a point of type (b) it will maintain the same direction which it has on either side of the considered point.

The direction of movement of the u-point will also be maintained, a fortiori, as x passes through any point where

$$d^2X/dx^2 \neq 0.$$

In the neighbourhood of such a point a unique Legendre dual transformation $x \leftrightarrow u$ can be constructed, which expresses the unique local inverse of the mapping (1) as

$$x = dU/du \tag{4}$$

in terms of a dual generating function

$$U(u) = ux(u) - X[x(u)]. \tag{5}$$

The transformation also has the property

$$d^2X/dx^2 . d^2U/du^2 = 1 \tag{6}$$

and so the procedure is reversible.

Such a Legendre transformation is valid, in the first instance, within any x-domain bounded by points satisfying (2), and there will be a corresponding u-domain. Beyond this x-domain boundary (or boundaries, at either end) there will be other x-domains, leading to different u-domains and corresponding different branches of the dual function $U(u)$. However, as x passes through any boundary point which is of type (b), i.e. one which does not specify an inflexion point of $X(x)$ and for which the corresponding u-point maintains its direction, the two adjacent branches of $U(u)$ can be matched in value and slope from opposite sides of their common u-domain boundary. The second derivatives become infinite by (2) and (6), but the slopes match because of (4) and the contiguity of the two x-domains.

For this reason the *convention* is now introduced that any pair of x-domains which are adjacent at a point of type (b) are counted as two parts of the *same enlarged* domain, and the matched pair of branches of $U(u)$ are counted as a *single* branch over the single u-domain formed by glueing together the previous abutting pair. By this convention a non-inflexion point which satisfies (2) is in future counted as an interior point of an associated Legendre domain.

This leaves the following situation. Equation (2) is a polynomial equation having at most $n-1$ real roots. Those roots which specify inflexion points of $X(x)$ divide the real x-axis into at most n contiguous domains $D_{x1}, D_{x2}, \ldots, D_{xn}$ (say). As the x-axis is traversed from $-\infty$ to $+\infty$, the sign of the curvature of $X(x)$ will *alternate* with each succeeding domain, changing only at the inflexion points. Within each domain the curvature will not change sign, being either convex or concave.

If n is odd there will be 1 or 3 or ... or n such x-domains, whereas if n is even there will be 2 or 4 or ... or n of them. The sketches in Figs. 1–4 illustrate those domains for the cases $n = 1, 2, 3, 4$.

As the x-axis is traversed, the succession of domains $D_{x1}, D_{x2}, \ldots$, will give a succession of distinct branches $U_1(u), U_2(u), \ldots$ of the composite Legendre dual function

$$\{U_1(u), U_2(u), \ldots\} \equiv W(u) \quad \text{(say)},$$

https://doi.org/10.1017/S0305004100053779 Published online by Cambridge University Press

each branch being defined over an associated u-domain $D_{u1}, D_{u2}, \ldots$ to be determined. A good qualitative picture of the way these branches fit together can be built up on the basis of three simple observations:

(1) Each u-domain must be traversed in the opposite sense to the preceding one, and therefore every pair of contiguous u-domains must overlap on the whole of at least one of them. This follows from equation (1) and property (a) above.

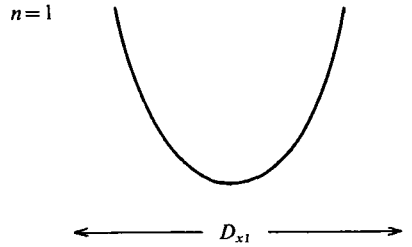


Fig. 1. One curvature domain D_{x1} for $X = \frac{1}{2}x^2$.

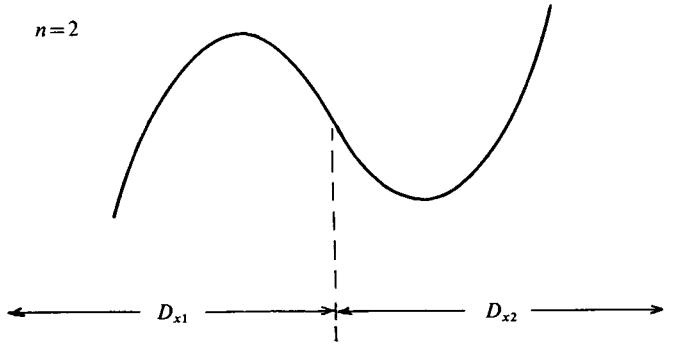


Fig. 2. Two curvature domains for $X = \frac{1}{3}x^3 + \frac{1}{2}ax^2$.

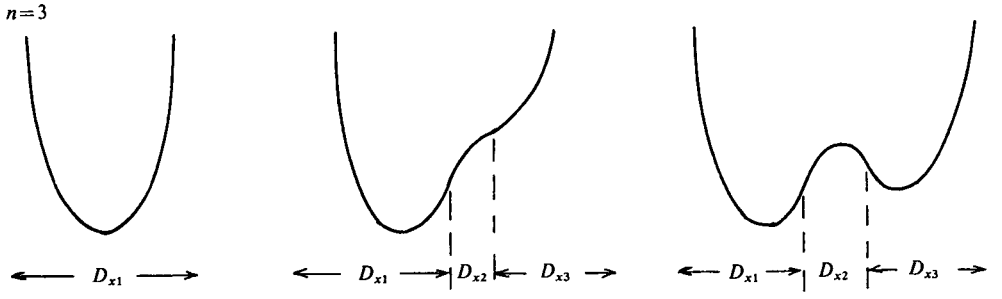


Fig. 3. One or three curvature domains for $X = \frac{1}{4}x^4 + \frac{1}{3}bx^3 + \frac{1}{2}ax^2$.

(2) The slope of succeeding distinct branches of $W(u)$ is continuous at their join. This follows from equation (4) and the contiguity of successive x-domains. (It is also true for points of type (b), a fact already utilized in the above convention.)

(3) The curvature of succeeding distinct branches of $W(u)$ alternate in sign, because this property holds for $X(x)$ (see Figs. 1–4), and convexity (or concavity) is transmitted from one generating function to its dual in a Legendre transformation.

https://doi.org/10.1017/S0305004100053779 Published online by Cambridge University Press

These observations are employed in Figs. 5–8 to sketch the qualitative form of the composite Legendre transforms $W(u)$ of the functions $X(x)$ shown in Figs. 1–4. In these diagrams no attempt is made to give the quantitative effects of all the different possible combinations of the parameters a, b, c (for example, to change the sign of a in

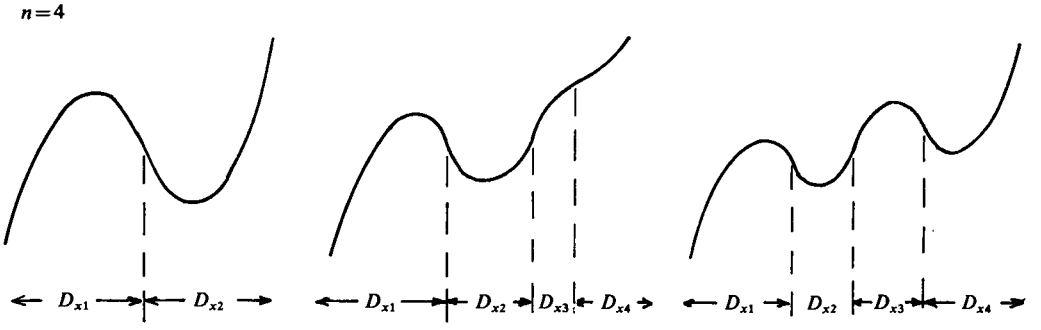


Fig. 4. Two or four curvature domains for $X = \frac{1}{5}x^5 + \frac{1}{4}cx^4 + \frac{1}{3}bx^3 + \frac{1}{2}ax^2$.

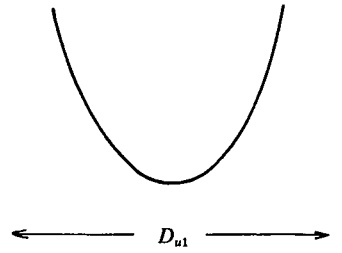


Fig. 5. One domain D_{u1} of $U = \frac{1}{2}u^2$ dual to Fig. 1.

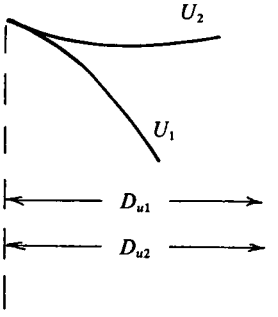


Fig. 6. Two overlapping domains of dual $W(u) = \{U_1, U_2\}$ to Fig. 2.

Fig. 2 will tilt the cusp of Fig. 6 downwards instead of upwards). The purpose here is to convey the qualitative features which can be deduced about the juxtaposition of the domains and branches of the composite Legendre transform $W(u)$, on the basis of the foregoing three observations. Succeeding branches of $W(u)$ always join at cusps.

Finally it may be noticed that if $X(x)$ is any sufficiently smooth function, not necessarily a polynomial, then as x passes through any point satisfying (2), the two

https://doi.org/10.1017/S0305004100053779 Published online by Cambridge University Press

Legendre transforms $U_i(u)$, $U_{i+1}(u)$ defined on either side by (5) have continuous value and slope at the considered point. Locally therefore, if the considered x-point is an inflexion of $X(x)$ (i.e. of type (a)), the two branches of the composite transform are defined over overlapping domains and meet in a cusp; whereas if it is not an inflexion

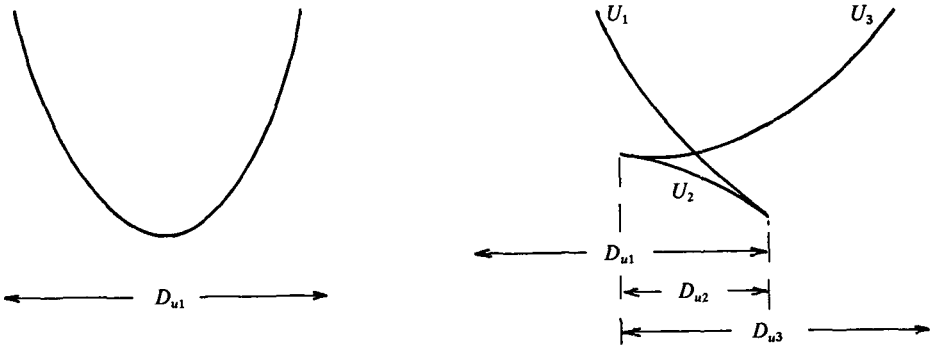


Fig. 7. One or three overlapping domains of dual $W(u) = \{U_1, U_2, U_3\}$ to Fig. 3.

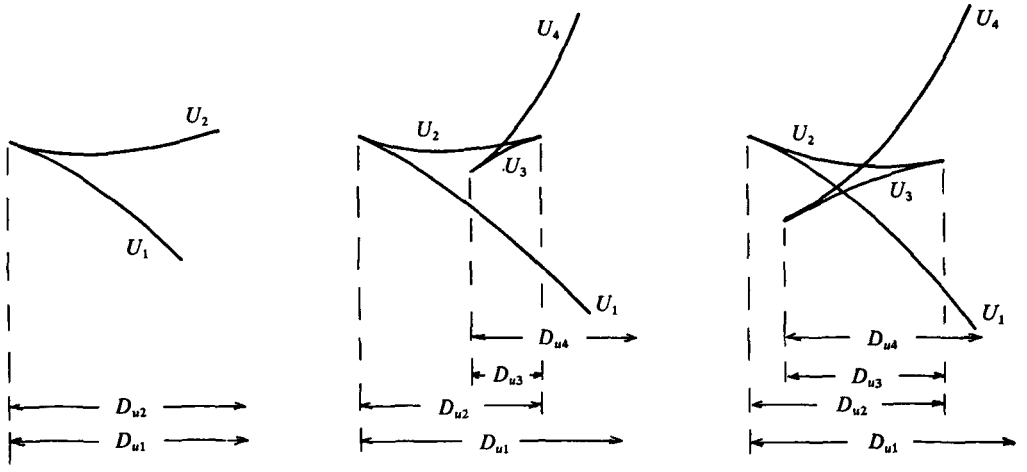


Fig. 8. Two or four overlapping domains of dual $W(u) = \{U_1, U_2, U_3, U_4\}$ to Fig. 4.

(i.e. type (b)) the two branches are defined over abutting domains and can be glued together to look like one branch. The cusp can never point straight upwards, nor can the composite transform have a vertical tangent, by (4) for finite x.

3. *Some elementary catastrophes.* It can be immediately recognized that the composite Legendre dual functions $W(u)$ portrayed in Figs. 6, 7 and 8 are qualitatively the same as at least certain cross-sections of the bifurcation sets of the cusp, swallowtail and butterfly elementary catastrophes respectively – see, e.g., §5·3 of Thom's book (9) for pictures of the latter.

A complete statement of the Legendre transformation beginning from the above polynomial

$$X(x; a, b, \ldots, t)$$

https://doi.org/10.1017/S0305004100053779 Published online by Cambridge University Press

takes account of the fact that the coefficients $a, b, \ldots, t$ play the role of passive variables. They therefore enter each branch

$$U_i(u; a, b, \ldots, t)$$

of the composite dual function

$$W = W(u; a, b, \ldots, t) \tag{7}$$

and have the properties

$$\frac{\partial X}{\partial a} + \frac{\partial U_i}{\partial a} = \frac{\partial X}{\partial b} + \frac{\partial U_i}{\partial b} = \ldots = \frac{\partial X}{\partial t} + \frac{\partial U_i}{\partial t} = 0$$

for each U_i. In future $\partial/\partial x$ is also used in place of the d/dx of section 2 and $\partial/\partial u$ in place of d/du.

A significant feature of the dual function (7) is that it depends only on the coefficients or 'controls' present in an associated potential function

$$\begin{aligned} V(x; a, b, \ldots, t, u) &= X - ux \\ &= \frac{1}{n+1}x^{n+1} + \frac{t}{n}x^n + \ldots + \frac{b}{3}x^3 + \frac{a}{2}x^2 - ux, \end{aligned} \tag{8}$$

in terms of which the starting point (1) of the Legendre transformation can be written

$$\partial V/\partial x = 0. \tag{9}$$

In mechanical contexts where V is potential energy depending on displacement x, with various possible interpretations for the control parameters, (9) defines, in the space of x and the parameters, an 'equilibrium surface' as introduced by Sewell (7, 8). Therefore (1) also defines this surface.

Two simple examples of the dual function $W(u)$ are now displayed explicitly.

Example 1: fold → cusp. If V in (8) is the universal unfolding for the fold catastrophe, then the corresponding

$$X = \tfrac{1}{3}x^3. \tag{10}$$

Then (1) generates $u = x^2$, and (2) and (3) hold at $x = 0$ with $r = 3$, corresponding to the (horizontal) inflexion in the cubic. The origin divides the x-axis into two domains $D_{x1} : x < 0$ and $D_{x2} : x > 0$. The inverses of $u = dX/dx$ in these domains are $x = -u^{\frac{1}{2}}$ and $x = u^{\frac{1}{2}}$ respectively, both branches being defined over the same domain

$$D_{u1} = D_{u2} : u > 0$$

of the u-axis. The associated composite Legendre transform is thus

$$W = \{U_1(u), U_2(u)\}, \quad U_1 = -\tfrac{2}{3}u^{\frac{3}{2}}, \quad U_2 = \tfrac{2}{3}u^{\frac{3}{2}}. \tag{11}$$

The two dual generating functions X and W in this Legendre transform are sketched in Fig. 9. This is a special case of Figs. 2 and 6. Evidently either branch of the dual function (11) satisfies

$$4u^3 - 27(W/\sqrt{3})^2 = 0.$$

This is the bifurcation set of *another* potential which is the cusp catastrophe unfolding

$$P(\xi; u, W) = \tfrac{1}{4}\xi^4 - \tfrac{3}{2}\lambda^2 u\xi^2 + 3\lambda^3 W\xi. \tag{12}$$

https://doi.org/10.1017/S0305004100053779 Published online by Cambridge University Press

Here λ is an arbitrary scale factor and ξ is some other behaviour variable identifiable as λx. This can be verified directly, or inferred from (34) and (35) below. One of the controls in (12) is the original one u, and the second control W is the Legendre transform generated by the original fold potential.

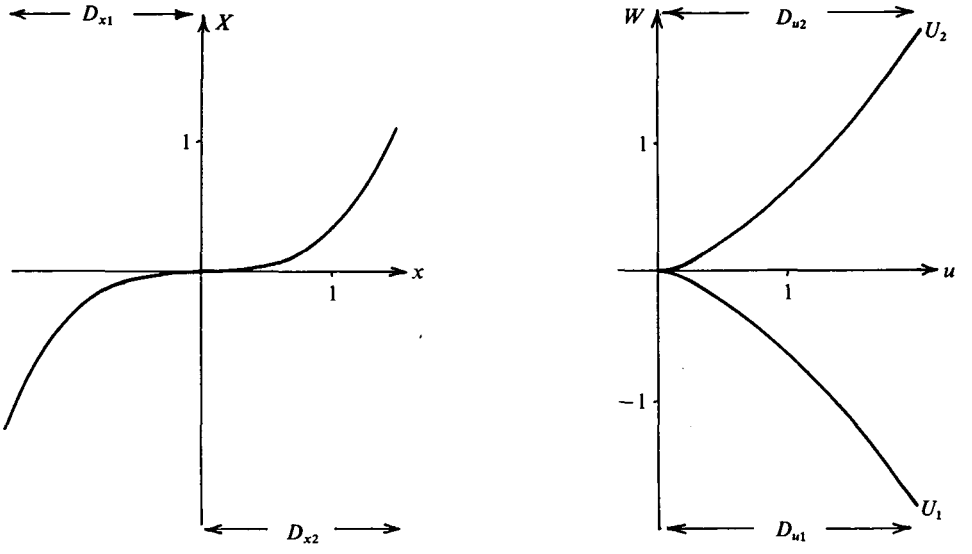


Fig. 9. Fold potential ↔ cusp dual.

Example 2: cusp→swallowtail. This time suppose that V in (8) is the universal unfolding for the cusp catastrophe. The term of penultimate highest power is therefore absent again. (Potentials with this property are associated with singularities called cuspoids.) For X this implies the *partial* unfolding

$$X = \tfrac{1}{4}x^4 + \tfrac{1}{2}ax^2 \tag{13}$$

as the starting point $X(x; a)$ of the Legendre transformation. Therefore (1) becomes

$$u = x^3 + ax, \tag{14}$$

which defines the familiar smooth folded equilibrium surface in x, a, u space (e.g. fig. 11 of Sewell (8), or the numerous illustrations by Zeeman, e.g. Isnard and Zeeman (2)). Then the limits of single-valued inverse branches of (14) are defined by (2), namely

$$3x^2 = -a, \tag{15}$$

because (3) holds with $r = 3$ (except at the single point $x = 0$). If $a > 0$ there is no such real limit to x, i.e. the quartic (13) has no inflexion, and over the whole x-axis there is a unique real solution $x = x(u, a)$ to the cubic. This inverse has the gradient $x = \partial U/\partial u$ of the unique Legendre transform

$$U(u; a) = \tfrac{3}{4}ux(u, a) - \tfrac{1}{4}a[x(u, a)]^2 \tag{16}$$

defined over the whole u-axis. The first diagrams in each of Figs. 3 and 7 give the qualitative picture.

https://doi.org/10.1017/S0305004100053779 Published online by Cambridge University Press

If $a < 0$, however, two real turning-points of the cubic (14) separate three contiguous x-domains

$$D_{x1}: -\infty < x < -(-\tfrac{1}{3}a)^{\frac{1}{2}},$$

$$D_{x2}: -(-\tfrac{1}{3}a)^{\frac{1}{2}} < x < (-\tfrac{1}{3}a)^{\frac{1}{2}},$$

$$D_{x3}: (-\tfrac{1}{3}a)^{\frac{1}{2}} < x < +\infty,$$

where (14) gives solutions $x_1(u, a)$, $x_2(u, a)$, $x_3(u, a)$ respectively. We do not need their explicit form here. Substituting each in turn into the same formula (16) already derived for the case $a > 0$ leads to three distinct branches

$$U_1(u;a) \quad \text{in} \quad D_{u1}: -\infty < u < -\frac{2a}{3}(-\tfrac{1}{3}a)^{\frac{1}{2}},$$

$$U_2(u;a) \quad \text{in} \quad D_{u2}: +\frac{2a}{3}(-\tfrac{1}{3}a)^{\frac{1}{2}} < u < -\frac{2a}{3}(-\tfrac{1}{3}a)^{\frac{1}{2}},$$

$$U_3(u;a) \quad \text{in} \quad D_{u3}: +\frac{2a}{3}(-\tfrac{1}{3}a)^{\frac{1}{2}} < u < +\infty,$$

of the composite Legendre transform

$$W(u;a) = \{U_1(u;a), U_2(u;a), U_3(u;a)\}. \tag{17}$$

The appropriate qualitative pictures this time are the last diagrams in each of Figs. 3 and 7, but symmetrized with respect to both horizontal and vertical axes because of the absence of the cubic 'bias' term in (13).

Consider now what happens when the passive variable a is allowed to vary. The most significant part of the surface (13) is displayed in Fig. 10 by computing its cross-sections a = constant and x = constant. The latter are straight lines with slope $\frac{1}{2}x^2$. The former are quartics with inflexions whose locus, for successive a-values, is also shown on Fig. 10. This locus has the parabolic projection (15) on the x, a plane, separating D_{x2} (for each a) from D_{x1} and D_{x3}.

The induced domain boundaries in the (u, a) plane calculated above lie on the familiar cusped curve

$$4a^3 + 27u^2 = 0 \tag{18}$$

(because the calculation defining them is equivalent to eliminating x from

$$\partial V/\partial x = \partial^2 V/\partial x^2 = 0 \quad \text{for} \quad V = \tfrac{1}{4}x^4 + \tfrac{1}{2}ax^2 - ux,$$

i.e. it is equivalent to calculating the bifurcation set for the cusp catastrophe).

The composite Legendre transform

$$W = W(u;a), \tag{19}$$

is a surface in three dimensions when both the active variable u and the passive variable a are allowed to vary. This is computed from (16) for $a > 0$, and from (17) for $a < 0$, and its most significant part is displayed in Fig. 11 via its successive cross-sections a = constant. Hidden portions are indicated by broken lines. To obtain the best display in the Figs. 10 and 11 it was necessary to use rather different viewpoints and a-ranges. The key point is that cross-sections of Figs. 10 and 11 with each given

https://doi.org/10.1017/S0305004100053779 Published online by Cambridge University Press

plane a = constant are Legendre transforms of each other, and the pictures show how these transforms vary with the passive variable a.

It is evident that Fig. 11 is of the same qualitative type as the bifurcation set for the swallowtail catastrophe. As a decreases through the origin, the surface retains its single-valued character only outside the cusped curve (18), while within it (i.e. over the

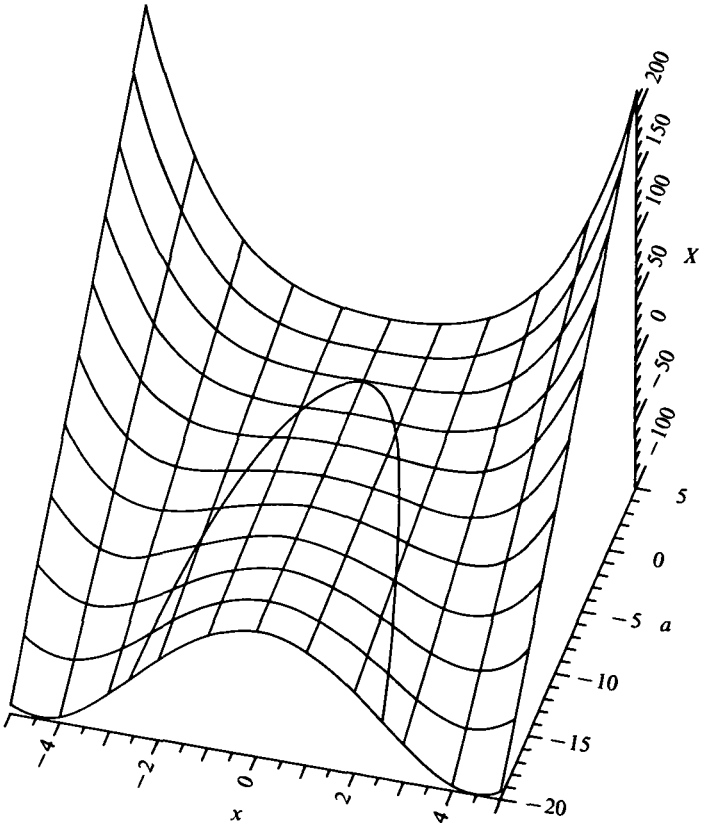


Fig. 10. Surface $X = \frac{1}{4}x^4 + \frac{1}{2}ax^2$ and locus of inflexions.

domain $27u^2 < -4a^3$, $a < 0$) the surface (19) becomes triple-valued. The middle concave branches in Figs. 10 and 11 map into each other. So do the outer left and right convex branches *respectively*, but with overlap over the central cusp-shaped domain.

The local shape of (19) near the cusp point $u = a = W = 0$ itself is hidden in Fig. 11. This is displayed in Fig. 12 by removing the right-hand halves $u > 0$ of the *upper* two branches of the surface, and using a slightly different viewpoint. Not only is the cusp-shaped boundary of the middle branch (having projection (18)) more clearly seen; but the cusped nature of the vertical section

$$W = W(0; a)$$

is also revealed. The latter is where the intersection of the two upper branches meets the a-axis $u = W = 0$, which lies in the lower branch. Analytically this vertical section

https://doi.org/10.1017/S0305004100053779 Published online by Cambridge University Press

through the plane of symmetry is the parabolic cusp

$$W = -\tfrac{1}{4}a[x(0,a)]^2 = \begin{cases} 0 & (-\infty < a < \infty) \\ \tfrac{1}{4}a^2 & (-\infty < a \leqslant 0), \end{cases} \tag{20}$$

just by putting $u = 0$ in (14) and (16). This is exactly the type of cusp which appears in the bifurcation set for the swallowtail (see Thom (9), p. 65).

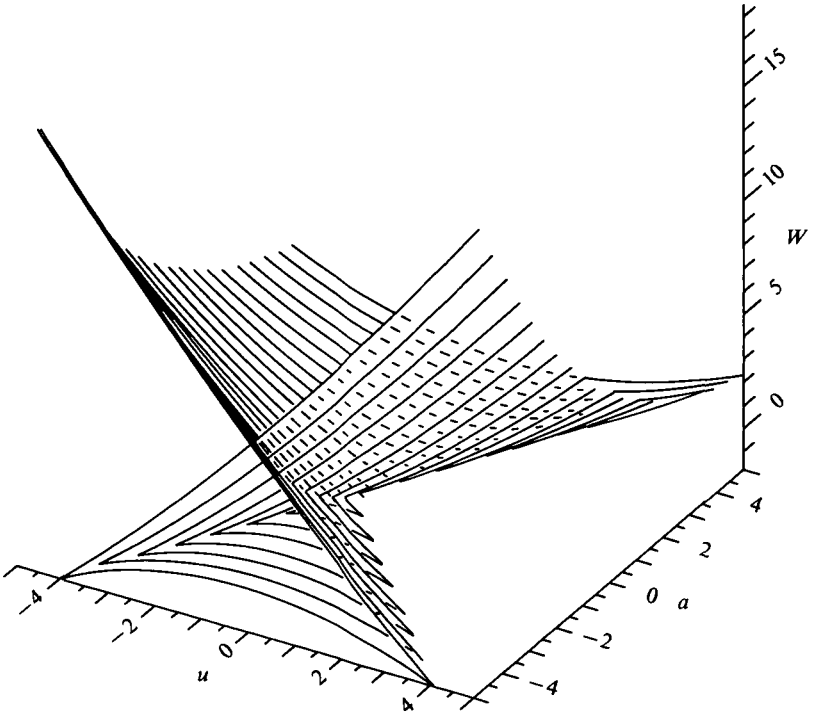


Fig. 11. Legendre transform $W = W(u; a)$ of Fig. 10.

In fact these findings can be summed up by the remark that if one begins with (13) (Fig. 10) and computes its composite Legendre transform (19) with passive a, this surface displayed in Fig. 11 is exactly the same as the bifurcation set of *another* potential which is the swallowtail catastrophe unfolding

$$P(\xi; a, u, W) = \tfrac{1}{5}\xi^5 + \tfrac{2}{3}\lambda^2 a\xi^3 - \lambda^3 u\xi^2 + 4\lambda^4 W\xi \tag{21}$$

for another behaviour variable $\xi = \lambda x$, where $\lambda \neq 0$ is any scale factor. The reason is that the two calculations are equivalent as can be seen directly or from (34) and (35) below. Two of the controls in (21) are the original u and a in (8) (for $n = 3$ with $b = 0$ so that (9) $\Rightarrow$ (14)), while the third control W is the Legendre transform W generated by the partial unfolding (13) of the cusp catastrophe.

We investigate the shape of Fig. 11 a little more closely. Every branch $U_i(u; a)$ of (19) has gradients $\partial U_i/\partial u = x$ and $\partial U_i/\partial a = -\frac{1}{2}x^2$. Every branch of the solution $x(u, a)$

https://doi.org/10.1017/S0305004100053779 Published online by Cambridge University Press

of the cubic (14) has the properties $\partial x/\partial u = 1/(3x^2+a)$ and $\partial x/\partial a = -x/(3x^2+a)$. Therefore each branch of (19) has second derivatives

$$\frac{\partial^2 U_i}{\partial u^2} = \frac{1}{3x^2+a}, \quad \frac{\partial^2 U_i}{\partial u \partial a} = -\frac{x}{3x^2+a}, \quad \frac{\partial^2 U_i}{\partial a^2} = \frac{x^2}{3x^2+a} \tag{22}$$

and so the 2×2 determinant

$$\left| \frac{\partial^2 U_i}{\partial(u, a)} \right| = 0 \tag{23}$$

on every branch. Formulae (22) are directly expressed in terms of the inside or outside of the locus of inflexions on Fig. 10. It follows that the upper two branches of Fig. 11

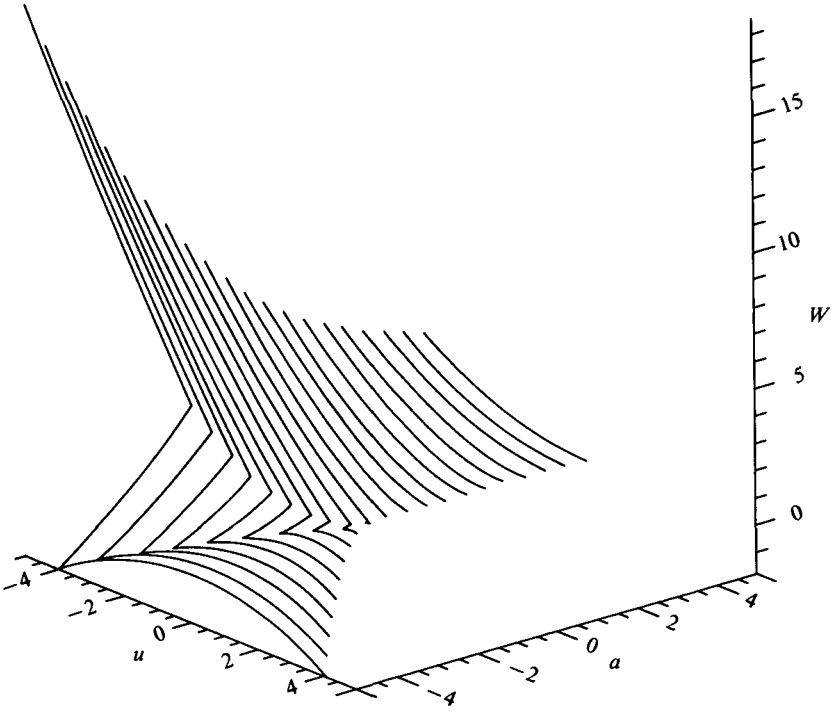


Fig. 12. Half $u > 0$ of upper branches removed from Fig. 11.

are strictly convex in u and a separately, but only weakly jointly convex in them (this applies in particular where the upper branches merge in $a > 0$). The lower middle branch $U_2(u; a < 0)$ is strictly concave in both variables separately, but only weakly jointly concave in them.

It also follows from (23) that through every point of the surface of Fig. 11, there is a curve in the surface along which the Gaussian curvature is zero. The local direction of the projection of this curve onto the u, a base plane is given by the eigenvector associated with the zero eigenvalue of (23), namely $du/da = x = \partial U_i/\partial a$. In other words it is given (from (14)) by the solution of

$$\left(\frac{du}{da}\right)^3 + a\frac{du}{da} - u = 0$$

https://doi.org/10.1017/S0305004100053779 Published online by Cambridge University Press

appropriate to the considered branch. In fact each plane section x = constant of Fig. 10 maps into a plane section $u = ax + x^3$ of Fig. 11. This satisfies the differential equation and so the desired projection is a straight line. As x is altered parametrically these lines envelop the cusped domain boundary (18), and their points of tangency

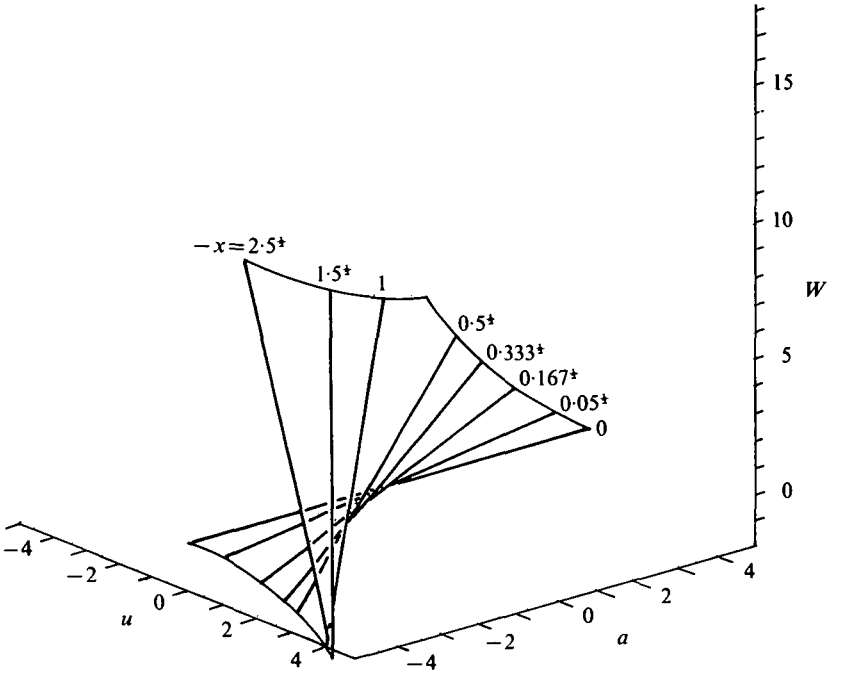


Fig. 13. Ruled surface segment of Legendre transform Fig. 11.

with that envelope correspond to where the straight sections x = constant in Fig. 10 cross the locus of inflexions there. The curves along which the Gaussian curvature of Fig. 11 is zero are therefore actually straight lines in three dimensions,

$$u - x^3 = \frac{a}{1/x}, \quad W - \tfrac{3}{4}x^4 = \frac{a}{2/x^2}, \tag{24}$$

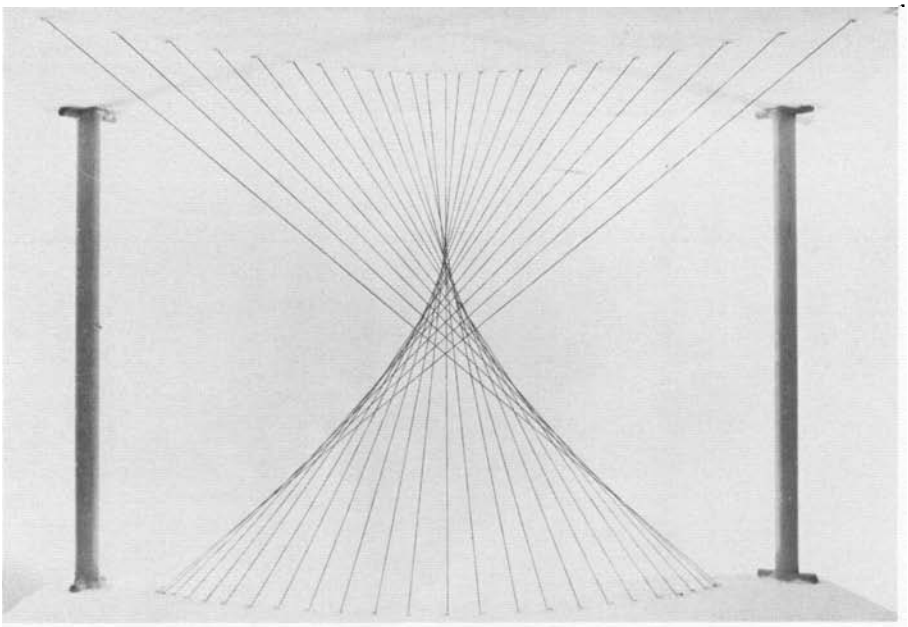
for each fixed x. The surface (19) in Fig. 11 could therefore have been displayed alternatively entirely as a ruled surface in terms of these straight lines, which transfer from an upper to the lower branch of the surface at their tangency points with the 'edge of regression'

$$W = -\tfrac{3}{4}x^4, \quad u = -2x^3, \quad a = -3x^2. \tag{25}$$

The latter is displayed in Fig. 11 as the boundary between the lower and upper branches of the Legendre transform. It is the mapping of the locus of inflexions of Fig. 10.

Fig. 13 displays (part of) Fig. 11 as a ruled surface, generated from successive straight lines (24) by altering the parameter x. In order that the picture should not be self-obscuring, we have selected only a limited set of x-values between 0 and $-2{\cdot}5^{\frac{1}{2}} = -1{\cdot}58$, and plotted the lines from the same viewpoint and in the same 'box' as in Fig. 12. The lines envelop the edge of regression (25) and touch it at a-values 0,

https://doi.org/10.1017/S0305004100053779 Published online by Cambridge University Press



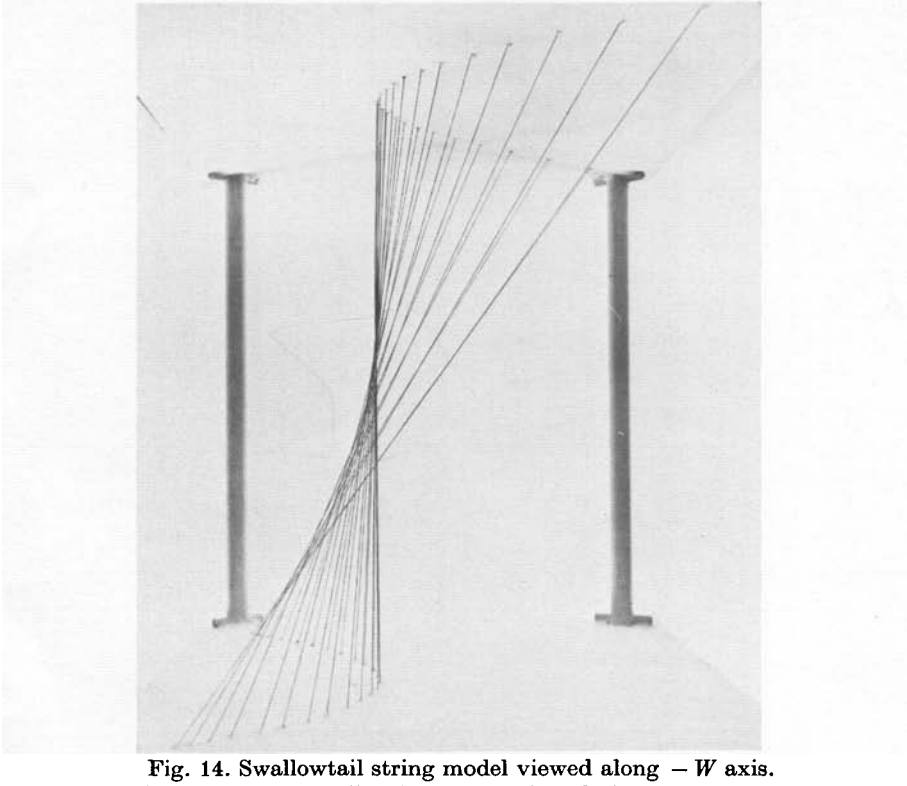


Fig. 14. Swallowtail string model viewed along $-W$ axis.
Fig. 15. Swallowtail string model viewed along $+u$ axis.

https://doi.org/10.1017/S0305004100053779 Published online by Cambridge University Press

$-0{\cdot}15, -0{\cdot}5, -1, -1{\cdot}5, -3, -4{\cdot}5, -7{\cdot}5$. Fig. 13 therefore shows how the Legendre transform maps certain straight-line sections $x =$ constant of Fig. 10, in the range

$$-1{\cdot}58 \leqslant x \leqslant 0$$

into straight-line sections of Fig. 11.

The photographs in Figs. 14 and 15, plate 1, show two orthogonal views of a string model of the swallowtail surface (24). The a-axis is vertically upward, and the floor and ceiling of the model are the planes $a = -5$ and $a = 2{\cdot}5$ respectively. One is looking

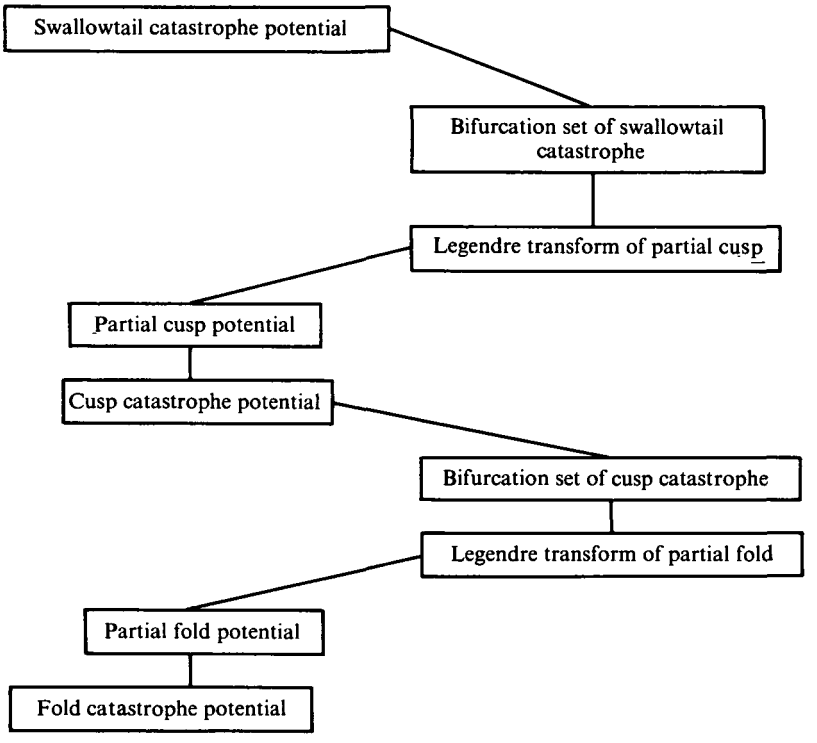


Fig. 16. A ladder for the cuspoids.

along the negative W-axis in Fig. 14 and the positive u-axis in Fig. 15. On each string x is a constant, and this value varies at intervals of 0·1 in the range $-1{\cdot}2 \leqslant x \leqslant 1{\cdot}2$ to generate successive strings. The outer limits on x are chosen such that the floor just avoids showing the section which it makes with the regressing second and third branches (these appear clearly in Fig. 11). The practical reason for this is to avoid drilling partly coalescing holes with a finite diameter drill – this can happen on the regressing branch of a cusp. The slight irregularities seen in the photographs arise because the string diameter is less than the hole diameter.

4. *A ladder for the cuspoids.* The results from the two examples of section 3 can be presented as the chain of connexions illustrated in Fig. 16. This expresses the hierarchy of elementary catastrophes in a way different from any that I have seen before. On the right in Fig. 16 are surfaces entirely in control spaces, while on the left one behaviour

https://doi.org/10.1017/S0305004100053779 Published online by Cambridge University Press

variable also appears in each potential. For example, from a cusp catastrophe potential (12) we can pass down the ladder to the fold potential $V = \frac{1}{3}x^3 - ux$, or (after altering the notation to identify the first two terms of (12) with (13)) up the ladder to a swallowtail potential. Each of the bifurcation sets may also be associated with many behaviour variables in the sense of the general qualitative equivalence theorem of catastrophe theory.

To give a general proof that the ladder of Fig. 16 can be extended up any number steps, it is convenient to rewrite the potential (8) as

$$V_n(\xi; a_n, \ldots, a_1) = \frac{1}{n+1}\xi^{n+1} + \sum_{r=1}^{n} \frac{1}{r} a_r \xi^r. \tag{26}$$

The subscript n is attached to V_n for emphasis, and when $a_n = 0$ we may call V_n the nth cuspoid potential (cf. Woodcock and Poston (10)). The fold $V_2 = \frac{1}{3}\xi^3 + a_1\xi$ is the second cuspoid after the trivial $\frac{1}{2}\xi^2$. The bifurcation set of (26) is the surface in the a_r-parameter space obtained by eliminating ξ from $\partial V_n/\partial\xi = 0$ and $\partial^2 V_n/\partial\xi^2 = 0$, i.e. from

$$\xi^n + \sum_{r=1}^{n} a_r \xi^{r-1} = 0,$$

and

$$n\xi^{n-1} + \sum_{r=2}^{n} (r-1) a_r \xi^{r-2} = 0.$$

Eliminating a_2 from the first of these, and rewriting the resulting equations in reverse order, gives

$$-a_2 = n\xi^{n-1} + \sum_{r=3}^{n} (r-1) a_r \xi^{r-2}, \tag{27}$$

$$a_1 = (n-1)\xi^n + \sum_{r=3}^{n} (r-2) a_r \xi^{r-1}. \tag{28}$$

Thus the bifurcation set is found in principle by eliminating ξ between these two equations.

On the other hand, if we begin with the potential V_{n-1} of degree one less than (26), and write it in the form

$$V_{n-1}(x; b_{n-1}, \ldots, b_1) = \frac{1}{n}x^n + \sum_{r=1}^{n-1} \frac{1}{r} b_r x^r, \tag{29}$$

its 'equilibrium equation' $\partial V_{n-1}/\partial x = 0$ can be expressed as the starting point

$$-b_1 = \frac{\partial X}{\partial x} \tag{30}$$

of a Legendre transformation generated by

$$X(x; b_{n-1}, \ldots, b_2) = \frac{1}{n}x^n + \sum_{r=2}^{n-1} \frac{1}{r} b_r x^r. \tag{31}$$

Then (30) is

$$-b_1 = x^{n-1} + \sum_{r=2}^{n-1} b_r x^{r-1}. \tag{32}$$

The Legendre transform $W(-b_1; b_{n-1}, \ldots, b_2)$ itself is obtained by inserting the succes-

https://doi.org/10.1017/S0305004100053779 Published online by Cambridge University Press

sive branches of the solutions x of (32) into $W = -b_1 x - X$. By (31) and (32) this has the values of

$$W = \frac{n-1}{n} x^n + \sum_{r=2}^{n-1} \left(\frac{r-1}{r} \right) b_r x^r. \tag{33}$$

The Legendre transform is thus obtainable in principle by eliminating x between (32) and (33).

The pair of equations (27) and (28) can be identified precisely with the pair of equations (32) and (33) if we introduce an arbitrary non-zero scale factor λ such that

$$\xi = \lambda x \tag{34}$$

and then match the coefficients according to the formulae

$$a_1 = n\lambda^n W, \quad a_{r+1} = \frac{n}{r} \lambda^{n-r} b_r, \quad 1 \leqslant r \leqslant n-1. \tag{35}$$

This establishes the desired *general theorem*: that the bifurcation set obtained in the n-dimensional a_r-space from (26) is the same as the Legendre transform

$$W = W(-b_1; b_{n-1}, \ldots, b_2) \tag{36}$$

generated with active x from (31) in the n-dimensional space spanned by W and the b_r, provided only that the trivial scaling (35) is applied to the n axes.

In particular the result holds for the cuspoid potentials in which $a_n = 0$ in (26) and $b_{n-1} = 0$ in (29). Woodcock and Poston (10) have computed the bifurcation sets for all the first seven cuspoids (i.e. up to $n = 7$ in (26) with $a_n = 0$), in terms of various ruled surface projections parametrized by ξ = constant. The same pictures are therefore immediately available as explicit illustrations of the multi-valued Legendre transform (36) generated from (31).

5. *A mechanical interpretation.* The general theorem, or the ladder of Fig. 16, can be interpreted as setting up a certain sequence of correspondences between different conservative systems.

For example, the two-bar frame analysed by Koiter (4), or the spring model examined by Budiansky (1), have a total potential energy of the type

$$V_2 = \tfrac{1}{3}x^3 + \tfrac{1}{2}b_2 x^2 + b_1 x,$$

where x is buckling deflection, b_2 is applied load and b_1 is imperfection. The bifurcation set of this model is the relation between imperfection and buckling load

$$b_1 = \tfrac{1}{4}b_2^2. \tag{37}$$

This is a parabola in b_1-, b_2-space displaying imperfection-sensitivity of the type first analysed by Koiter (3) – i.e. a small (second-order) change in imperfection permits a large (first order) decrease in buckling load.

Stepping first to the bottom step of the ladder (not shown in Fig. 16, but see Sewell (8), p. 169) (37) is *also* the relation between a weight $(1/\sqrt{2})\, b_2$ suspended in equilibrium

https://doi.org/10.1017/S0305004100053779 Published online by Cambridge University Press

from a Hookean spring, and the complementary energy b_1 of the spring. For when the extension of the spring is x, the total normalized potential energy of the system is

$$V_1 = \tfrac{1}{2}x^2 - \frac{1}{\sqrt{2}}b_2 x,$$

its internal energy is $\frac{1}{2}x^2$, and the Legendre transform of this is the complementary energy having the value $\frac{1}{4}b_2^2$ in equilibrium.

Now stepping up the ladder from the fold-type potential V_2, we can regard its 'partial form' $\frac{1}{3}x^3 + \frac{1}{2}b_2 x^2$ as the potential energy of the perfect version of the stated structure. The Legendre transform of this is the complementary energy W of the perfect version. The values of this when the imperfect structure is in equilibrium have the same dependence

$$W = \tfrac{2}{3}[-\tfrac{1}{2}b_2 \pm (\tfrac{1}{4}b_2^2 - b_1)^{\frac{1}{2}}]^3 + \tfrac{1}{2}b_2[-\tfrac{1}{2}b_2 \pm (\tfrac{1}{4}b_2^2 - b_1)^{\frac{1}{2}}]^2 \qquad (38)$$

as does the bifurcation set of the new quartic structure

$$V_4 = \tfrac{1}{4}x^4 + \tfrac{1}{2}b_2 x^3 + \tfrac{3}{2}b_1 x^2 + 3Wx.$$

This fact can be read off from (26) and (35) with $n = 3$ and $\lambda = 1$.

Geometrical non-linearities frequently induce quartic potentials in engineering structures, and if we change the origin of the behaviour variable here by writing $x = y - \frac{1}{2}b_2$ we convert this potential into

$$V_4 = \tfrac{1}{4}y^4 - \tfrac{3}{2}y^2[\tfrac{1}{4}b_2^2 - b_1] + y[\tfrac{1}{4}b_2^3 - \tfrac{3}{2}b_1 b_2 + 3W] + \text{constant}.$$

By comparison with similar expressions given by Sewell(8) for compressed struts and shallow arches, we can identify the coefficients here with geometry variables, loads and imperfections whose buckling values are related by (38).

By constructing the Legendre transform of the internal energy (or of the 'perfect' energy) of such quartic structures with linear terms omitted we can arrive at the bifurcation set of another structure with swallowtail potential, and so on.

These remarks about elastic systems give some preliminary colouring to the general theorem. The unfoldings of elementary catastrophe theory are currently based on finite-dimensional hypotheses. They serve, like a new telescope, to reveal or bring into focus the target of certain infinite-dimensional investigations, without in themselves improving the weapons available for hitting that target. Many targets have been hit in the past without the aid of such a telescope, especially in elasticity; some have not, and some have not been known to exist. But a clearer view of the target may stimulate methods of hitting it. A problem of intermediate generality can arise in which the *ab initio* behaviour variables are not scalars but are second order tensors x_{ij} (say, perhaps subject to constraint, for example like that implied for stresses by balancing moment of momentum). We have in mind the question of whether Thom's theorem can be applied to problems of the type

$$\partial V/\partial x_{ij} = 0$$

to give an explicit list of unfoldings of tensor polynomials informing the study of 'material stability'. Even the concept of complementary energy itself has not been without ambiguity in non-linear elasticity until very recently, as papers by Koiter(5) and Ogden(6) show.

https://doi.org/10.1017/S0305004100053779 Published online by Cambridge University Press

The views of surfaces in three dimensions shown in Figs. 10–12 were computed during my tenure of a Visiting Professorship at the Mathematics Research Center, University of Wisconsin, with support from the United States Army under contract no. DAAG29-75-C-0024. I am indebted to Barry Finkel for carrying out the computer graphics, and to Mr I. Maclean of Reading University for taking the photographs.

REFERENCES

(1) Budiansky, B. Theory of buckling and post-buckling of elastic structures. *Advances in Applied Mechanics* **14** (1974), 1–65.

(2) Isnard, C. A. and Zeeman, E. C. Some models from catastrophe theory in the social sciences. In *Use of models in the social sciences*, ed. L. Collins (London, Tavistock, 1974).

(3) Koiter, W. T. On the stability of elastic equilibrium. *NASA Technical Translation F*–10, 833, 1967. (Translation of a 1945 Thesis in Dutch.)

(4) Koiter, W. T. Post-buckling analysis of a simple two-bar frame. In *Recent progress in applied mechanics* (The Folke Odqvist Volume), pp. 337–354 (Wiley, 1966).

(5) Koiter, W. T. On the complementary energy theorem in non-linear elasticity theory. In *Trends in applications of pure mathematics to mechanics*, ed. G. Fichera, pp. 207–232. (London, Pitman, 1976).

(6) Ogden, R. W. Inequalities associated with the inversion of elastic stress-deformation relations and their implications. *Math. Proc. Cambridge Philos. Soc.* **81** (1977), 313–324.

(7) Sewell, M. J. On the connexion between stability and the shape of the equilibrium surface. *J. Mech. Phys. Solids* **14** (1966), 203–230.

(8) Sewell, M. J. Some mechanical examples of catastrophe theory. *Bulletin of the Institute of Mathematics and its Applications* **12** (1976), 163–172.

(9) Thom, R. *Structural stability and morphogenesis* (Reading, Mass., W. A. Benjamin, Inc., 1975).

(10) Woodcock, A. E. R. and Poston, T. *A geometrical study of the elementary catastrophes* (Berlin, Springer-Verlag, 1974).

Note added in proof: Van der Waals' equation relating normalized pressure p, temperature t and specific volume v can be written as $p = -\partial\psi/\partial v$ in terms of the free energy

$$\psi = v - \frac{3}{v} - \frac{8}{3}(t+1)\log(3v-1).$$

For given negative t near enough to the liquid/gas 'critical point' $(p, t, v) = (0, 0, 1)$, the function $\psi[v]$ is a non-polynomomial example of the middle of Fig. 3 above. It follows from the methods of this paper that the free enthalpy $\zeta[p]$ will look like the second of Fig. 7 (but upside down) at the given t, since $v = \partial\zeta/p$ by the Legendre transformation connecting the thermodynamic potentials. As a clear-cut convention for the suppression of super-heating and super-cooling, one may propose that the centre hump of the ψ-surface be removed and replaced by the common 'supporting' tangent plane needed to make the surface weakly convex. Correspondingly the swallowtail part of the ζ-surface would be excised, leaving the volume jump at the change of state to be given by the slope discontinuity at the self-intersection point. This is to be compared with existing conventions like that of Maxwell or 'equal areas'. Other examples of 'Degenerate duality, catastrophes and saddle functions' are described in my lectures to a 1977 Summer School on 'Duality and complementarity in mechanics of solids', Polish Academy of Sciences, Warsaw.

https://doi.org/10.1017/S0305004100053779 Published online by Cambridge University Press